Clays and Clay Minerals, Vol. 22, pp. 155–165. Pergamon Press 1974. Printed in Great Britain

ELECTRON-OPTICAL INVESTIGATIONS ON MONTMORILLONITES—I. CHETO, CAMP-BERTEAUX AND WYOMING MONTMORILLONITES

NECIP GÜVEN

Department of Geosciences, Texas Tech University,
P.O. Box 4109, Lubbock, Texas 79409, U.S.A.

(*Received* 19 *March* 1973)

Abstract—Other layer silicates are consistently present as impurities in natural montmorillonite samples. They have a distinctly different morphology from the common montmorillonite particles. The selected area electron diffraction (SAD) of these impurities display unusually sharp spot patterns with triclinic, monoclinic and hexagonal symmetries. These impurities are most likely micas, which are easily detectable with X-rays in the coarser fractions ($> 10\ \mu m$) of the samples.

The crystal structure model with the space group C2 for montmorillonite single layer has an unusual configuration of OH's and vacancies for a dioctahedral layer silicate. Our intensity calculations do not bring a conclusive evidence for distinguishing the two possible space groups C2 and C2/*m* on the observed SAD patterns of montmorillonite.

The SAD of the thin montmorillonite flakes in Cheto, Camp-Berteaux and Wyoming samples display uniform ring, circular arcs and spotty ring patterns, respectively. These patterns indicate different modes of association of crystallites or different arrangements of elementary layers within them.

INTRODUCTION

In this report the term 'montmorillonite' is used as the name for the specific dioctahedral smectite. This clay mineral forms the major component in the rocks called 'bentonite' and therefore, is the most common smectite in nature. It has a wide range of applications in various fields of industry, agriculture and engineering. For most of these applications, the following basic properties of this clay mineral are important:

(1) Crystal structure

(2) Crystal morphology: particle habit, size and the nature of surface atomic planes

(3) Mode of associations of crystallites.

Electron optics offer appropriate methods for the investigations of these properties. The combination of selected area electron diffraction (SAD) with the transmission electron image provides the most powerful method for this purpose. Major contributions along this line were made by the late Professor Mering and his associates. These contributions have been reviewed in two recent publications (Mering and Oberlin, 1967, 1971). Several other studies mentioned below have also been concerned with the electron diffraction properties of this clay mineral. The conclusions of these investigators regarding the crystal structure of the montmorillonite were, however, not quite in agreement. Results of our investigations, presented in the following discussion, may contribute to the explanation of the above discrepancy and also to the understanding of the real nature of montmorillonite particles.

RESULTS OF PREVIOUS ELECTRON DIFFRACTION STUDIES ON THE CRYSTAL STRUCTURE OF MONTMORILLONITE

Zvyagin and Pinsker (1949), using the 'oblique texture' method on polycrystalline specimens, proposed the space group C2/*m* for montmorillonite. This is the ideal symmetry of a mica-type layer silicate. They did not make any deductions regarding the details of the structure.

Cowley and Goswami (1961) published SAD patterns with hexagonal symmetries for montmorillonites from: Clay Spur, Wyoming; Little Rock, Arkansas; and New South Wales. They explained the hexagonal symmetry in terms of 20–50° bending of elementary montmorillonite layers. The bending was deduced from the Patterson syntheses of about 20 SAD reflections to which they assigned *hk*0 indices. They assumed that individual tetrahedral and octahedral networks independently scatter in order to generate a hexagonal symmetry. Furthermore, the SAD patterns published by Cowley and Goswami (1961) for one type of montmorillonite (Type B) look similar to those of impurities described below.

Mering and Oberlin (1967, 1971) obtained spot patterns in the following way: They separated fine frac-

tions from the bulk montmorillonite samples and saturated them with sodium. The specimen grids used for electron diffraction were unshadowed and thin particles were, therefore, invisible. Despite that, all their SAD patterns were unquestionably from montmorillonite particles. For the Wyoming sample they obtained a monoclinic spot pattern with the plane point group 2 *mm*. From this pattern, Mering and Oberlin (1967, 1971) concluded that the Wyoming montmorillonite single layer has the non-centrosymmetrical plane group c*l*m*l* (corresponding to space group C2). Similarly, they obtained SAD patterns with hexagonal symmetry from the Camp-Berteaux montmorillonite. These hexagonal patterns were interpreted by them as edge-to-edge associations of montmorillonite crystallites arranged with about 60° orientations.

Roberson and Towe (1972) recently reported SAD spot patterns with triclinic symmetries for Wyoming and Camp-Berteaux montmorillonites. They worked in the 'blind mode' like Mering and Oberlin; thus, they were not able to observe the images of the particles giving rise to the diffraction patterns. They assumed that the fine fractions of the montmorillonite samples were monomineralic and that all diffraction patterns belonged to the montmorillonite particles. This assumption may be questioned because of the possible presence of impurities.

ELECTRON–OPTICAL OBSERVATIONS ON MONTMORILLONITES

We have been carrying out extensive electron–optical investigations on bentonites from Professor R. E. Grim's bentonite collection, which includes a large number of type localities throughout the world. In the following discussion, electron–optical data will be described on samples from three occurrences. These localities are Cheto, Arizona (Collection Nr. 361); Camp-Berteaux, Morocco (Collection Nr. 177); and Wyoming (with Na as predominant interlayer cation), U.S.A. (Collection Nr. 357–C52).

The $<2\,\mu$m (e.s.d.) fractions of the samples were separated by centrifugation. A drop of the suspension containing this fraction was diluted to a clay concentration of a few ppm using a 700:1 mixture of water and tertiary butylamine (Serwatzky, 1962). This mixture has a pH of about 11 which considerably reduces particle aggregation as shown by McAtee *et al.* (1969). A drop of this dilute suspension was dried on a Formvar film, and the grid was coated with gold at a shadowing angle of about 26°. At this angle, the shadowing provides a rather practical measure of flake thickness because the length of the shadow is twice the thickness of the particle; however, folding of the particles may alter the shadow lengths. Of more importance, the shadowing process greatly increases the contrast of transmission images. The gold coating material also helps to give excellent contrast to the electron images of clay particles. After shadowing, very thin flakes were noticeable which, otherwise, were practically invisible.

A JEM-7 electron microscope, equipped with a completely variable field limiting aperture, was operated at 80 kV and the following observations were made.

CHETO MONTMORILLONITE

A typical aggregate of this sample is shown in Fig. 1(a) at an original magnification of 82,000 ×. SAD gives

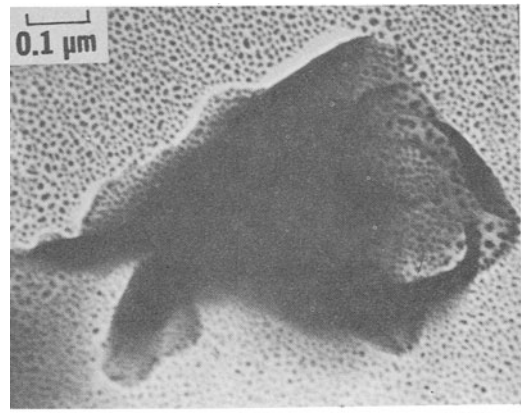

(a)

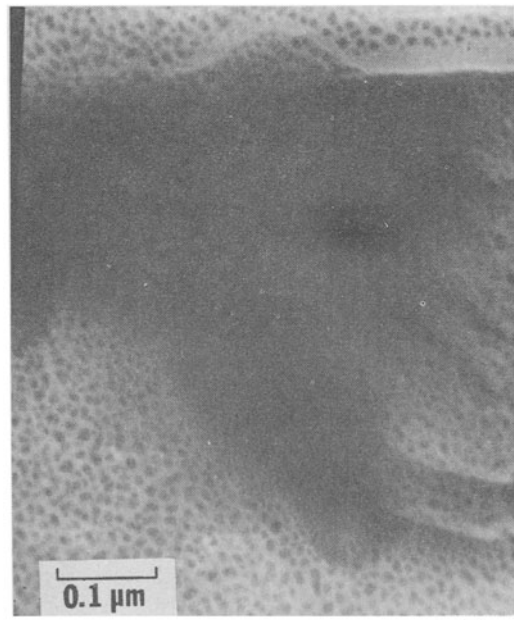

(b)

1. A typical montmorillonite aggregate with 'cotton texture' in the Cheto sample: (a) At a magnification of 82,000 ×, (b) At a magnification of 130,000 ×.

https://doi.org/10.1346/CCMN.1974.0220203 Published online by Cambridge University Press

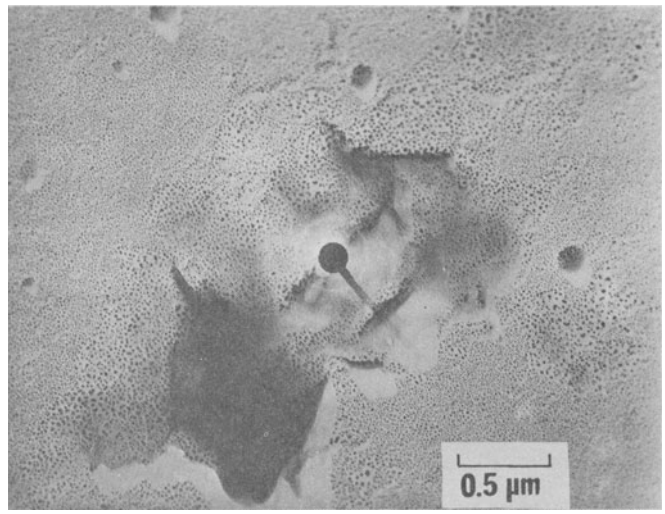

Fig. 2. Thin montmorillonite flake in the Cheto sample with its superimposed SAD patterns.

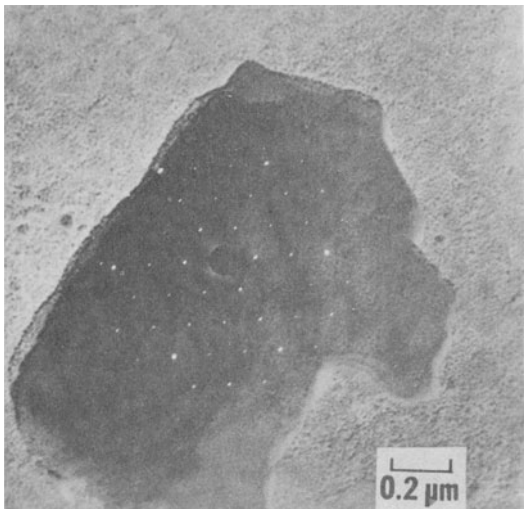

Fig. 3. A subhedral mica flake in the Cheto sample. Its SAD pattern, superimposed on the image, has been taken from a 0·5 μm^2 area in the central portion of the flake.

a uniform *hk* type ring pattern indicating the presence of a fine polycrystalline aggregate. Part of the same image is magnified up to 135,000 × in Fig. 1(b). The aggregate has a featherlike appearance which fans out with curled edges. The texture resembles a flattened cotton ball, and might, therefore, be called a 'cotton texture'. The shadows indicate a thickness of about 60 ± 10 Å in the thin areas where the shadow is not elongated due to the folding of the flake. The aggregate gives, however, the impression of being rather soft and flexible instead of a rigid solid. Another very thin flake of montmorillonite, shown in Fig. 2, has a larger flat portion although several folds are visible. The SAD pattern from this flat portion, superimposed on the previous image, shows a uniform *hk* type ring pattern. These observations may be interpreted in two ways: (a) A montmorillonite flake represents an aggregate of fine crystallites with random azimuthal orientations about their common c^* direction; and (b) A montmorillonite flake consists of a turbostratic sequence of elementary layers.

In addition to the above montmorillonites, there are impurities with distinctly different morphology from montmorillonite particles as seen on Figs. 3, 4(a) and 5. These impurities are very similar to fine mica flakes. They are not observed on the X-ray diffraction patterns of the $< 2\ \mu m$ fractions of the sample. The X-ray diffractograms of the coarser fractions ($> 10\ \mu m$) clearly show the presence of a mica with 10 Å basal spacing. These impurities are, therefore, tentatively identified as micas, and will be so referred to in the rest of the report. In some cases the impurity may well be kaolinite on chlorite. The exact identity is not necessary for the argument in this report. It is, however, important to realize the presence of these impurities. Such a mica, shown in Fig. 3, gives a SAD spot pattern with the symmetry of the plane point group 2 *mm*. An extremely thin mica particle (Fig. 4a) has a shadow of about 60 ± 10 Å long indicating a thickness of 30 ± 10 Å. The SAD pattern of this mica also displays the symmetry of the plane point group 2 *mm* (Fig. 4b). Finally, Fig. 5 shows the drastic difference between a mica flake and a montmorillonite flake of approximately same size. The mica is flat and extremely thin and it has a subhedral outline. The montmorillonite aggregate,

https://doi.org/10.1346/CCMN.1974.0220203 Published online by Cambridge University Press

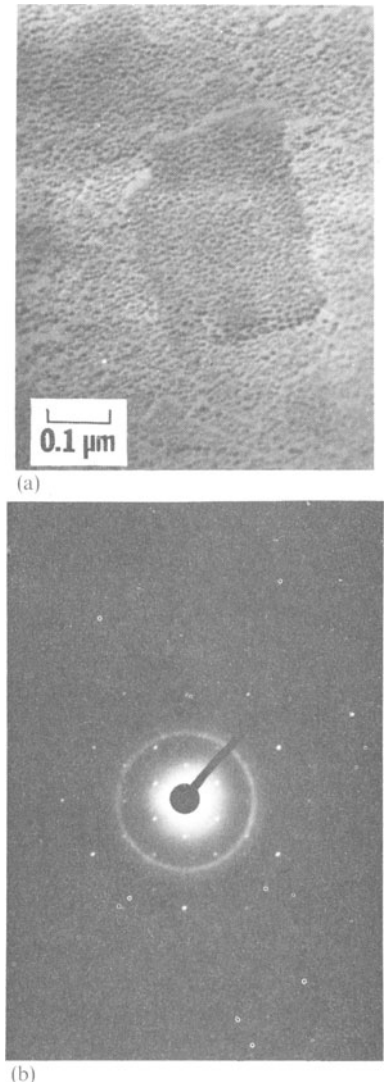

Fig. 4. A mica flake of about 30 Å thickness: (a) The transmission electron image at a magnification of 82,000 ×, (b) The SAD pattern of the mica in Fig. 4(a). Note that uniform rings belong to the gold coating material.

on the other hand, is rather thick and irregular with folds and curls.

CAMP-BERTEAUX MONTMORILLONITE

This montmorillonite has been extensively studied by the investigators mentioned earlier. In the following discussion, the emphasis will be placed on the impurities in the sample which do not seem to have been considered previously. In the $<2\ \mu m$ fraction of the samples there are minor amounts of mica flakes which were not detected by X-ray diffraction determinations.

Fig. 5. Typical thin and subhedral mica, and a rather thick and irregular montmorillonite aggregate in the Cheto sample.

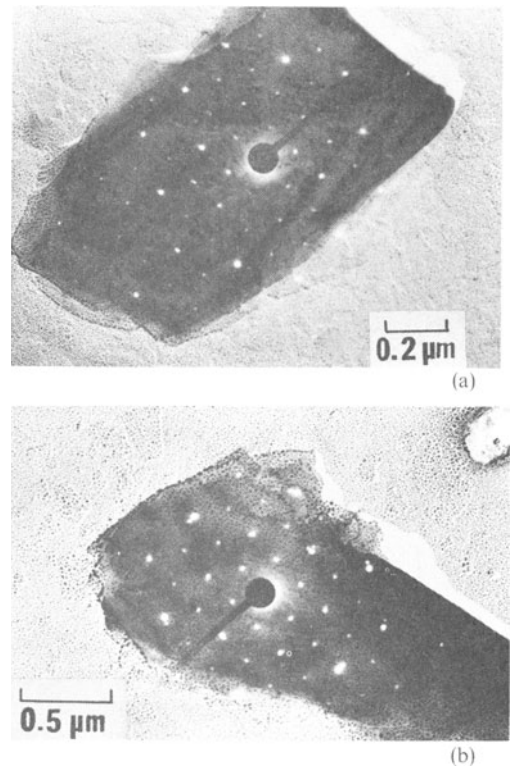

Fig. 6. Transmission electron images of micas with their superimposed SAD patterns in the Camp-Berteaux sample: (a) A mica flake with the plane point symmetry 2; (b) Another mica flake with hexagonal symmetry in SAD pattern.

https://doi.org/10.1346/CCMN.1974.0220203 Published online by Cambridge University Press

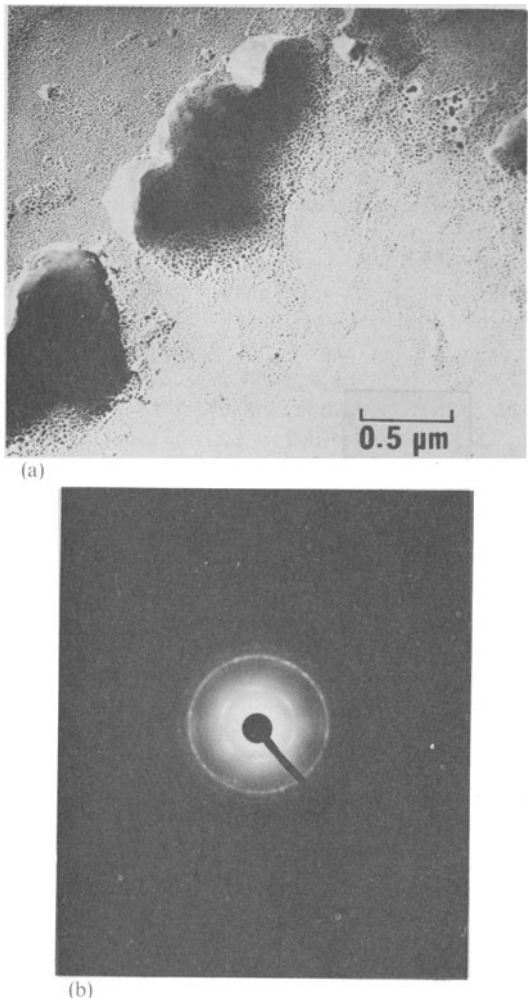

Fig. 7. Typically folded and irregular montmorillonite aggregates in the Camp-Berteaux sample: (a) the transmission electron image; (b) the SAD pattern of the thin aggregate in Fig. 7(a).

But these micas often come under the electron beam and give sharp SAD spot patterns. Such a mica flake is shown in Fig. 6(a), where the SAD pattern is also superimposed on the image. The symmetry of the SAD pattern is strictly the plane point group 2 indicating a triclinic symmetry. A similar SAD pattern was published by Roberson and Towe (1972) for the Camp-Berteaux montmorillonite. They assigned the diffraction pattern to a single montmorillonite layer.

Another mica flake in the sample displays hexagonal symmetry on the SAD pattern with the plane point group 6 *mm* or very close to it (Fig. 6b). Similar micas are also present in much smaller sizes and thinner flakes. Some of them display the point group 2 *mm* in SAD patterns, indicating a monoclinic symmetry; others show triclinic or hexagonal symmetry. These different SAD symmetries may be related to the stacking sequence or to experimental factors described elsewhere (Güven, 1974). Typical montmorillonite flakes seem to be irregular aggregates with folds and curled edges as seen in Fig. 7(a). The SAD pattern of the thin flake in Fig. 7(a) shows circular arcs (Fig. 7b) indicating preferred azimuthal orientations of fine crystallites or elementary layers along [11], [02], [1$\bar{1}$], in addition to having a common c* direction. In Fig. 8(a), we see the contrast between a montmorillonite aggregate and micas in the sample. Montmorillonite

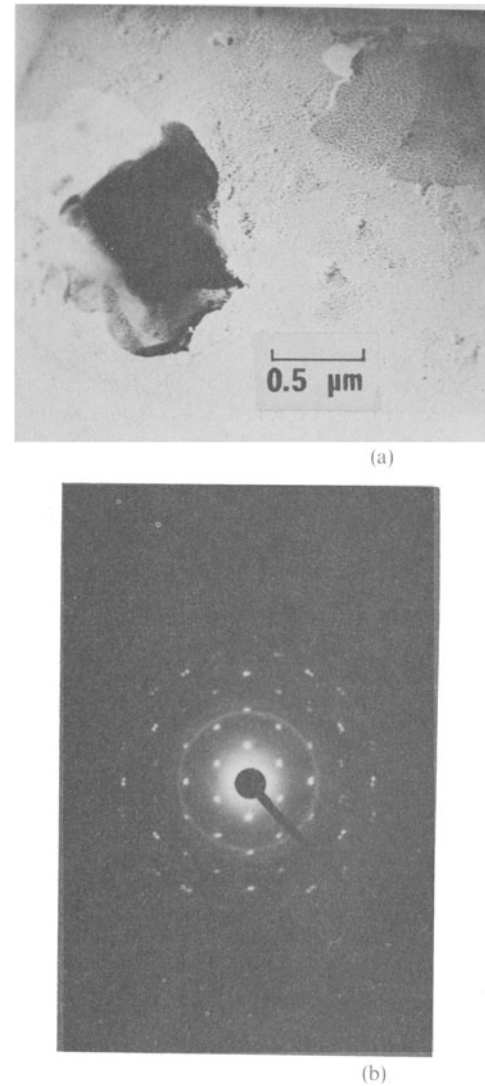

Fig. 8. Thin, edge-to-edge associated mica flakes, and thick, folded montmorillonite aggregate in the Camp-Berteaux sample: (a) transmission electron image; (b) the SAD pattern of micas in Fig. 8(a). Note that uniform rings belong to the gold coating material.

https://doi.org/10.1346/CCMN.1974.0220203 Published online by Cambridge University Press

Fig. 9. The transmission electron image of a thin, flat aggregate of crystallites in the Wyoming montmorillonite.

appears as a folded and curled aggregate whereas the mica flakes are very thin and flat. The SAD pattern of these micas (Fig. 8b) displays a hexagonal symmetry with some of the spots slightly separated like the flakes.

WYOMING MONTMORILLONITE

Wyoming montmorillonites display morphological features that are distinct from those of the Cheto and Camp-Berteaux montmorillonites. They seem to have crystallites with larger dimensions up to 0·5 μm (Fig. 9) and they form rather flat flakes. Irregular folding of the flakes and curling of the edges are still present but to a smaller extent.

A typical montmorillonite flake is shown in Fig. 9 at an original magnification of about 42,000 ×. The SAD pattern of the very-thin, upper-left, flat portion of the flake gives spotty ring pattern similar to that described below. The formation of discrete spots along the rings indicates that montmorillonite crystallite size is appreciably increased. Furthermore, the stacking of the elementary layers in each crystallite can no longer be turbostratic (i.e. completely random about the layer normal). They may have definite azimuthal orientations possibly without a regular sequence. A turbostratic stacking would be expected to give uniform diffraction rings on SAD pattern.

Figure 10(a) shows three types of particles: a thin, flat one (*D*), a thicker one (*T*), and two larger folded aggregates (*A*). SAD of the thin particles (*D*) gives a spotty ring pattern. The thicker montmorillonite particle (*T*) gives also a spotty ring pattern (Fig. 10b) which may illustrate some of the complications with SAD of montmorillonite particles. The intensities for a set of spots, apparently from a single crystal, are much stronger than the other spots along the same diffraction ring. There are five distinct spots between the 02 and 11 reflections. Nine of such spots are, however, resolved between the 06 and 33 reflections. These additional weak spots along the rings may indicate the presence of several other smaller crystallites. The intensity distribution over the main spots of the apparently single crystal has a symmetry close to hexagonal for the 02, 11; 20, 13; and 06, 33 sets of reflections. The 04 reflection has stronger intensity than that of the 22 and $2\bar{2}$ reflections, which reduces the symmetry of the pattern to monoclinic. A similar SAD pattern with a clearer monoclinic symmetry was given by Mering and Oberlin (1967, 1971). They attributed this SAD pattern to the presence of montmorillonite single layers. The transmission electron image of the particle (*T* in Fig. 10a) giving rise to the SAD pattern in Fig. 10(b) shows at least three major individual crystallites in a somewhat trigonal arrangement. If these individuals were of equal volumes, the SAD pattern would be exactly hexagonal. Unequal volumes of crystallites or partial preferred orientation in stacking sequence of elemental layers within them may result in monoclinic or triclinic symmetry on the SAD pattern. Thus, the monoclinic

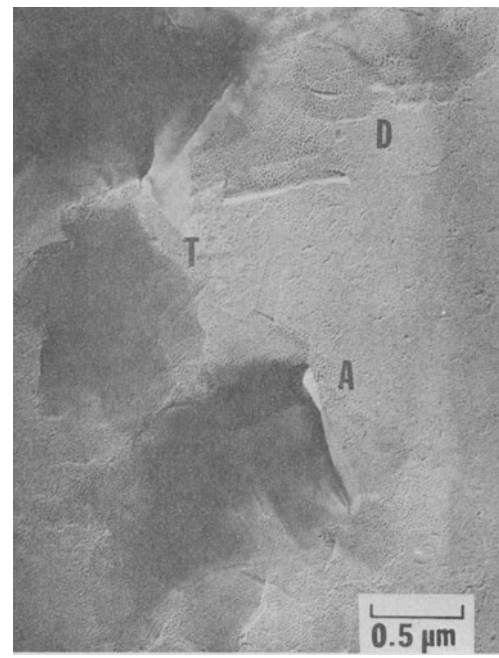

Fig. 10. Three types of Wyoming montmorillonites: (a) The transmission electron image, (*D*) Thin flat particles, (*T*): Thicker particle in the centre, (*A*): large folded aggregates.

https://doi.org/10.1346/CCMN.1974.0220203 Published online by Cambridge University Press

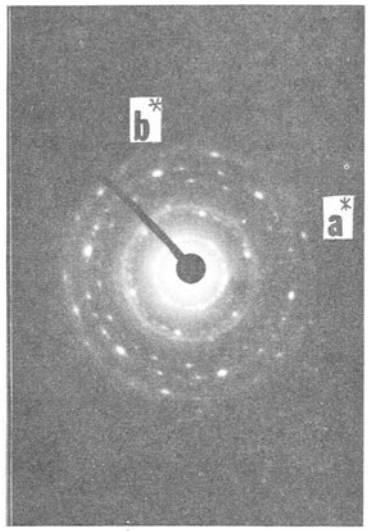

(b)

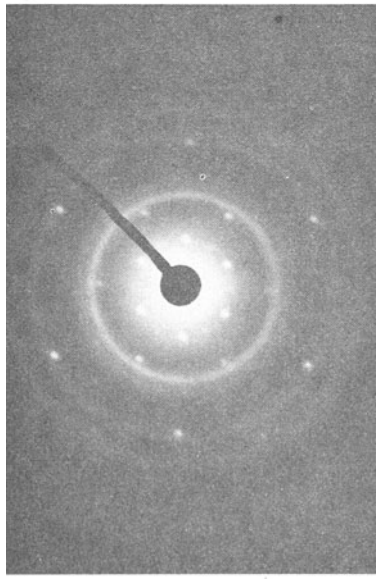

(c)

Fig. 10. Three types of particles in the Wyoming montmorillonite: (b) The SAD pattern of the particle (*T*) in Fig. 10a. (c) The SAD pattern of a very thin flake in the Wyoming sample (see text).

SAD pattern does not necessarily indicate the presence of a montmorillonite single layer as it was assumed by Mering and Oberlin (1967, 1971).

Although Wyoming montmorillonite seems to be a very suitable sample in which to isolate single crystals, we were not able to do so. Whenever we found a single crystal pattern while searching in the diffraction mode, it turned out to be a thin mica when we took a transmission electron image.

In a few instances, very thin flakes were observed, which gave a spot pattern (Fig. 10c) with a hexagonal symmetry. These flakes were so thin that their transmission electron images gave very poor contrast. Often these flakes are destroyed by the electron beam during SAD. It is really not possible to distinguish in this case whether these particles are montmorillonite or another layer silicate. In any case, the SAD pattern shows that the intensities of two spots, 11 and 02, are almost equal to each other and these are the strongest spots on the pattern.

STRUCTURE OF THE MONTMORILLONITE SINGLE LAYER

Mering and Oberlin (1967) concluded from their SAD studies that the montmorillonite single layer has the non-centrosymmetrical plane group c*m*l (corresponding to the space group C2). They also suggested that the structure may exhibit certain deviations from the ideal scheme similar to those observed in muscovite. In the following, the symmetry of montmorillonite will be discussed in terms of more familiar space group notations instead of plane groups. This approach also makes it unnecessary to consider the projections of the structures. The space group C2 presents certain rather unusual crystal-chemical features for a layer silicate. As is well known, there are two possible configurations of octahedral networks in dioctahedral micas. Figure 11a represents the common configuration with the ideal symmetry of C2/*m* for the space group (i.e. *c*2 *mm* for the plane group) where the mirror plane passes through OH's and vacant octahedral sites. This configuration is observed in all the well-studied dioctahedral micas where distortions and order–disorder may cause reduction of this symmetry to its subgroups C2, C$\bar{1}$, etc. The other configuration, shown in Fig. 11(b), has the C2 space group where the mirror plane is destroyed by the choice of vacant octahedral sites. An unusual feature of this configuration is the fact that the OH–OH edges, shown on the unshaded faces of the octahedra, are not shared between octahedral cations. There is an asymmetric distribution of anions around the vacant site. Such a hydroxyl configuration has not yet been observed in another dioctahedral layer silicate. The spatial relationships between hydroxyls and vacant sites seem to be rather important for the stability of a dioctahedral layer. As shown by Güven (1972) for Marblehead illite, the parting planes utilized during the breakdown of mica flakes pass through OH's and vacant octahedral sites. Furthermore, the relative displacement of tetrahedral sheets within a mica layer is

https://doi.org/10.1346/CCMN.1974.0220203 Published online by Cambridge University Press

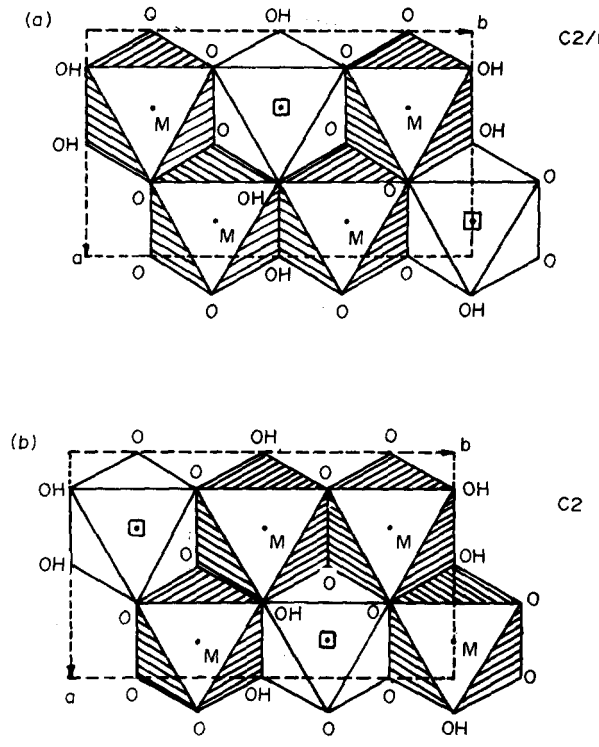

Fig. 11. Two octahedral configurations of dioctahedral micas projected along the normal to the layers: (a) the configuration with C2/*m* symmetry, (b) the asymmetrical configuration with C2 symmetry. Note the positions of vacancies ⊡ and OH's in both cases.

always parallel to the vector passing through OH's and vacant octahedral sites in projection. This may be a contributing factor in the stacking mechanism for a layer silicate.

Thus, the space group C2, if correct, gives rather unusual properties to the montmorillonite single layers as compared to the other dioctahedral mica-type layers.

INTENSITY CALCULATIONS FOR SAD PATTERNS OF A MONTMORILLONITE SINGLE LAYER

The method of intensity calculations for SAD patterns of crystals with 'finite' thickness has been presented elsewhere by Güven (1974). Intensity calculation for a crystal of single unit-cell thickness forms a limiting case of that method. In this case, the 'interference function' is unity along the *hk* rods parallel to c^* because there is only one unit-cell in this direction. The intensity is now a continuous function and it is determined by the $|F_{hkl}|^2$ where *l* indices can be a fraction as well as an integer. For these calculations, the montmorillonite single layer is referred to a monoclinic cell with dimensions $a = 5{\cdot}17$ Å, $b = 8{\cdot}95$ Å, $c = 10{\cdot}0$ Å and $\beta = 100°$. The atomic coordinates are derived from a well-determined 1 M type mica, namely phlogopite (Steinfink, 1962). For the space group C2/*m* of the dioctahedral montmorillonite the octahedral position in the center of symmetry has been left vacant. Similarly for the space group C2 one of the other two octahedral positions has been left unoccupied. The chemical composition of montmorillonite was considered to be $Na_{0{\cdot}33}(Al_{1{\cdot}67}Mg_{0{\cdot}33})Si_4O_{10}(OH)_2$.

The diffracted electrons originate from the portion of each *hk* rod in the vicinity of the Ewald sphere. This region is referred to as 'the excitation region'. Table 1 gives the ordinary *hkl* reflections in this region for several (*hk*) spots. The expected intensities $|F_{hkl}|^2$ of these reflections are also given in the same table for two possible space groups C2/*m* and C2. The continuous intensity distribution between these reciprocal lattice points is calculated by varying *l* indices with increments of $\Delta l = 0{\cdot}1$. The obtained intensity distributions are plotted in Fig. 12 for both space groups. In this figure, the $\zeta = 0$ plane determines exactly where the Ewald sphere intersects each *hk* rod. Under exact focusing conditions of the objective lens, the SAD pattern represents the section of the reciprocal lattice at $\zeta = 0$. Assuming there is no error in the focusing conditions, and disregarding the depth of field of the

https://doi.org/10.1346/CCMN.1974.0220203 Published online by Cambridge University Press

Table 1. Sections of *hk* rods in the 'excitation region'. Calculated intensities $|F_{hkl}|^2$ are only given at three reciprocal lattice points. The continuous intensity is plotted in Fig. 12; (ζ) is given in fraction of c^*

hk spot on SAD	Three r.l. points in the excitation region	ζ (Distance from the Ewald sphere)	$\lvert F_{hkl}\rvert^2$ (Normalized to $I_{13\bar{(0\cdot6)}=100}$) C2/*m*	C2
	0 2 1	0·99	1	8
02	0 2 0	−0·01	77	32
	0 2 $\bar{1}$	−1·01	1	8
	1 1 1	1·32	0	10
11	1 1 0	0·32	11	49
	1 1 $\bar{1}$	−0·68	34	10
	2 0 1	1·64	45	45
20	2 0 0	0·64	40	40
	2 0 $\bar{1}$	−0·36	17	17
	1 3 1	1·30	42	42
13	1 3 0	0·30	17	17
	1 3 $\bar{1}$	−0·70	41	41
	0 4 1	0·96	8	2
04	0 4 0	−0·04	1	7
	0 4 $\bar{1}$	−1·04	8	2
	2 2 0	0·63	0	6
22	2 2 $\bar{1}$	−0·37	7	2
	2 2 $\bar{2}$	−1·37	0	6
	2 4 0	0·60	2	1
24	2 4 $\bar{1}$	−0·40	4	10
	2 4 $\bar{2}$	−1·40	3	1
	3 1 0	0·93	1	5
31	3 1 $\bar{1}$	−0·07	10	4
	3 1 $\bar{2}$	−1·07	3	1
	1 5 1	1·26	2	7
15	1 5 0	0·26	1	6
	1 5 $\bar{1}$	−0·74	11	5
	0 6 1	0·91	11	11
06	0 6 0	−0·09	63	63
	0 6 $\bar{1}$	−1·09	11	11
	3 3 0	0·91	11	11
33	3 3 $\bar{1}$	−0·09	65	65
	3 3 $\bar{2}$	−1·09	10	10

objective lens (Güven, 1974), we may draw the following inference from the Fig. 12: The intensity variations along the *hk* rods indicate that only 02 and 11 reflections may have a diagnostic value in distinguishing these two space groups. This conclusion was also reached by Mering and Oberlin (1967, 1971) and these reflections were used in their choice of the space group C2 for the montmorillonite single layer.

The intensity ratio between 02 and 11 at $\zeta = 0$ (i.e. $l = 0{\cdot}0$ for 02 and $l = -0{\cdot}3$ for 11) is approx 3·3 for the space group C2/*m* and this ratio forms a definite criterion for this space group. Deviations from this ratio can be explained by the presence of multiple layers with stacking faults or with different stacking modes. For the space group C2, the I_{20}/I_{11} ratio at $\zeta = 0$ is found to be about 0·7 in this report and about 1·5 by Mering and Oberlin (1971). Discrepancy in this value may derive from different methods of calculation or from assumption of different models. In any case, the Mering and Oberlin's ratio ($I_{20}/I_{11} \cong 1{\cdot}5$) does not provide a dependable criterion for the space group C2 for the reasons mentioned above. The I_{20}/I_{11} ratio of 0·7, which is found in this paper, may have a diagnostic value. The observed data are $I_{20}/I_{11} = 1{\cdot}4$ (Mering and Oberlin, 1971) and $I_{20}/I_{11} \cong 1{\cdot}0$ in this report. Neither observation provides conclusive evidence for distinguishing between the space groups C2/*m* and C2.

CONCLUSIONS

The following points are emphasized:

1. The question has been raised whether SAD patterns of single montmorillonite layers have been actually observed.

https://doi.org/10.1346/CCMN.1974.0220203 Published online by Cambridge University Press

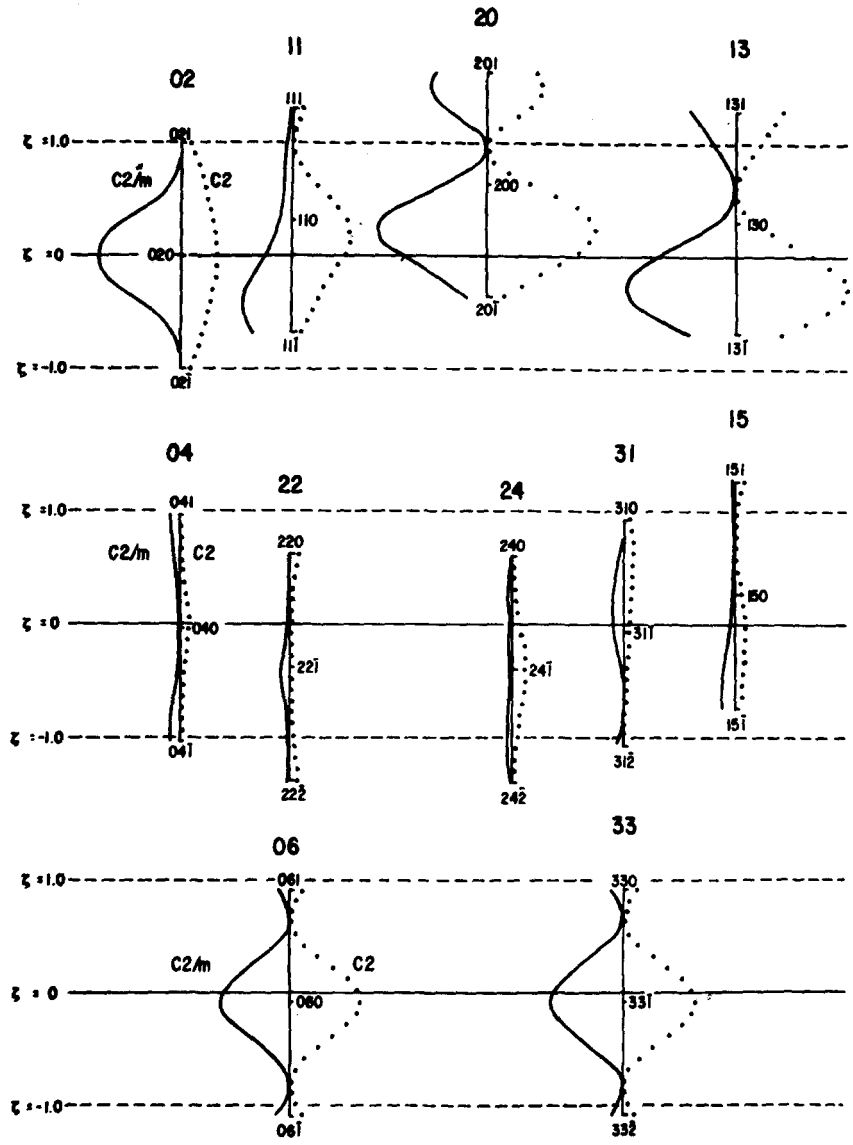

Fig. 12. Intensity distributions along the *hk* rods in the excitation region for a montmorillonite single layer. ζ-axis gives the distance of the reciprocal lattice points from the Ewald sphere and $\zeta = 0$ line determines the intersection of the *hk* rods with the same sphere. Intensity distributions are represented by solid line for the space group C2/*m* and by dotted lines for the space group C2.

2. We were not able to obtain montmorillonite SAD patterns which permit an unambiguous symmetry determination for this mineral. More work is needed in the future with proper consideration of the factors affecting SAD properties of layer silicates.

3. Finally, the reader is cautioned not to draw the conclusion from this report that montmorillonites do not give SAD spot patterns.

Acknowledgements—The author is deeply indebted to Prof. R. E. Grim for the most generous offer of his invaluable bentonite collection. Rodney W. Pease has patiently eliminated most of the grammatical errors in the original manuscript.

REFERENCES

Cowley, J. M. and Goswami, A. (1961) Electron diffraction patterns of montmorillonite: *Acta Crystallogr.* **14,** 1071–1079.

Güven, N. (1972) Electron-optical observations on Marblehead illite: *Clays and Clay Minerals* **20,** 83–88.

Güven, N. (1974) Factors affecting selected area electron diffraction patterns of micas: *Clays and Clay Minerals* **22,** 97–106.

McAtee, J. L., Jr. and Henslee, W. (1969) Electron microscopy of montmorillonite dispersed at various pH: *Amer. Mineral.* **54,** 869–874.

Mering, J. and Oberlin, A. (1967) Electron-optical study of smectites: *Clays and Clay Minerals* **15,** 3–25.

Mering, J. and Oberlin, A. (1971) The smectites: In *The Electron-Optical Investigation of Clays* (Edited by Gard, J. A.), pp. 193–229. Mineralogical Society Monograph 3, London.

Roberson, H. E. and Towe, K. M. (1972) Montmorillonite: Electron diffraction from two-dimensional single crystals: *Science* **176,** 908–909.

Serwatzky, G. (1962) Über die Präparation von Tonen für die electronoptische Untersuchung: *Sprechsaal* **21,** 559–565.

Steinfink, H. (1962) Crystal structure of a trioctahedral mica: phlogopite: *Amer. Mineral.* **47,** 886–896.

Zvyagin, B. B. and Pinsker, Z. G. (1949) Structure of montmorillonite: *C.R. Acad. Sci. URSS.* **68,** 65–67, 505–508.

Résumé—D'autres phyllosilicates que la montmorillonite sont présents normalement comme impuretés dans les montmorillonites naturelles. Ils ont une morphologie distinctement différente de celle des particules normales de montmorillonite. La microdiffraction électronique (SAD) de ces impuretés donne des taches inhabituellement nettes, relevant de symétries triclinique, monoclinique et hexagonale. Ces impuretés sont en général des micas facilement détectables avec les rayons X dans les fractions les plus grossières ($> 10\ \mu m$) des échantillons.

Le modèle de structure cristalline avec le groupe spatial C 2 pour le feuillet de montmorillonite a une configuration inhabituelle pour un phyllosilicate dioctaédrique, en ce qui concerne les OH et les lacunes. Nos calculs d'intensité n'apportent pas de preuve concluante pour distinguer les deux groupes spatiaux possibles, C 2 et C $2/m$ d'après les diagrammes de SAD observés avec les montmorillonites.

La SAD de fines lamelles de montmorillonites de Cheto, de Camp-Berteau et du Wyoming, montre respectivement des diagrammes en anneaux uniformes, en arcs circulaires et en anneaux ponctués. Ces diagrammes indiquent différents modes d'association des cristallites ou différents arrangements des feuillets élémentaires dans les cristallites.

Kurzreferat—In natürlichen Montmorillonitproben sind erklärlicherweise andere Schichtsilicate als Verunreinigungen enthalten. Sie besitzen eine von der der gewöhnlichen Montmorillonitteilchen deutlich unterschiedene Morphologie. Die Feinbereichselektronenbeugungsdiagramme (SAD) dieser Verunreinigungen weisen gewöhnlich scharfe Punktmuster mit trikliner, monokliner und hexagonaler Symmetrie auf. Diese Verunreinigungen bestehen sehr wahrscheinlich aus Glimmern, die leicht durch Röntgenbeugung in den gröberen Fraktionen ($> 10\ \mu m$) der Proben nachweisbar sind.

Das Kristallstrukturmodell mit der Raumgruppe C 2 für die Einzelschicht des Montmorillonits weist eine für ein dioktaedrisches Schichtsilicat ungewöhnliche Konfiguration der OH-Gruppen und der Fehlstellen auf. Unsere Intensitätsberechnungen erbringen keinen schlüssigen Nachweis für eine Unterscheidung der beiden möglichen Raumgruppen C 2 und C $2/m$ anhand der erhaltenen SAD-Diagramme des Montmorillonits.

Die SAD der dünnen Montmorillonitplättchen in Cheto-, Camp-Berteaux- und Wyoming-Proben weisen einförmige ring-bzw. kreisförmige Bogen- und fleckige Ringmuster auf. Diese Muster deuten auf eine unterschiedliche Art der Zusammenlagerung der Kristallite oder auf eine unterschiedliche Art der Anordnung der Elementarschichten innerhalb der Kristallite hin.

Резюме — В природных образцах монтмориллонита всегда присутствуют другие слоистые силикаты. Их частицы обладают заметно отличающейся морфологией от обычных частиц монтмориллонита. Электронная дифракционная картина избранной площади этих включений показывают необыкновенно резкие световые пятна с триклинной, моноклинной и шестиугольной симметриями. Эти включения весьма вероятно слюды, которые легко детектируются рентгеновскими лучами в более крупных фракциях ($>10\ \mu м$) образцов.

Модель структуры кристалла пространственной группы С2 одного слоя монтмориллонита имеет необыкновенную конфигурацию ОН и пустоты для диоктаэдрально слоистого силиката. Наши расчеты интенсивности не дали решающего доказательства для различения двух возможных пространственных групп С2 и С2/м на электронной дифракционной картине монтмориллонита.

Электронные дифракционные картины тонких чешук монтмориллонита в образцах из Чето, Камп-Берто и Вайоминга отображают однородные кольца, круговые арки и точечные изображения колец, соответственно. Эти рисунки указывают на различные формы ассоциации кристаллов или различное расположение их элементарных слоев.

https://doi.org/10.1346/CCMN.1974.0220203 Published online by Cambridge University Press